HHS Public Access

Author manuscript

Chemosphere. Author manuscript; available in PMC 2019 January 14.

Published in final edited form as:

Chemosphere. 2017 October ; 185: 983–990. doi:10.1016/j.chemosphere.2017.07.105.

Inhibitory effects of fifteen phthalate esters in human cDNA-expressed UDP-glucuronosyltransferase supersomes

Yun-Feng Cao[a], **Zuo Du**[b], **Zhi-Tu Zhu**[c], **Hong-Zhi Sun**[c], **Zhi-Wei Fu**[b,c], **Kun Yang**[b], **Yong-Zhe Liu**[b], **Cui-Min Hu**[d], **Pei-Pei Dong**[e,*], **Frank J. Gonzalez**[f], and **Zhong-Ze Fang**[b,**]

[a]Key Laboratory of Contraceptives and Devices Research (NPFPC), Shanghai Engineer and Technology Research Center of Reproductive Health Drug and Devices, Shanghai Institute of Planned Parenthood Research, Shanghai, China

[b]Department of Toxicology, School of Public Health, Tianjin Medical University, 22 Qixiangtai Road, Heping District, Tianjin, China

[c]Key Laboratory of Liaoning Tumor Clinical Metabolomics (KLLTCM), Jinzhou, Liaoning, China

[d]Tianjin Life Science Research Center, Department of Microbiology, School of Basic Medical Sciences, Tianjin Medical University, Tianjin, China

[e]Institute (college) of Integrative Medicine, Dalian Medical University, Dalian, China

[f]Laboratory of Metabolism, Center for Cancer Research, National Cancer Institute, National Institutes of Health, Bethesda, MD, United States

Abstract

Phthalate esters (PAEs) have been extensively used in industry as plasticizers and there remains concerns about their safety. The present study aimed to determine the inhibition of phthalate esters (PAEs) on the activity of the phase II drug-metabolizing enzymes UDP-glucuronosyltransferases (UGTs). *In vitro* recombinant UGTs-catalyzed glucuronidation of 4-methylumbelliferone was used to investigate the inhibition potentials of PAEs towards various s UGTs. PAEs exhibited no significant inhibition of UGT1A1, UGT1A3, UGT1A8, UGT1A10, UGT2B15, and UGT2B17, and limited inhibition of UGT1A6, UGT1A7 and UGT2B4. However, UGT1A9 was strongly inhibited by PAEs. *In silico* docking demonstrated a significant contribution of hydrogen bonds and hydrophobic interactions contributing to the inhibition of UGT by PAEs. The K_i values were 15.5, 52.3, 23.6, 12.2, 5.61, 2.79, 1.07, 22.8, 0.84, 73.7, 4.51, 1.74, 0.58, 6.79, 4.93,6.73, and 7.23 μM for BBOP-UGT1A6, BBZP-UGT1A6, BBOP-UGT1A7, BBZP-UGT1A7, DiPP-UGT1A9, DiBPUGT1A9, DCHP-UGT1A9, DBP-UGT1A9, BBZP-UGT1A9, BBOP-UGT1A9, DMEP-UGT1A9, DPP-UGT1A9, DHP-UGT1A9, DiBP-UGT2B4, DBP-UGT2B4, DAP-UGT2B4, and

*Corresponding author. Institute (college) of Integrative Medicine, Dalian Medical University, Dalian, China. **Corresponding author. Department of Toxicology, School of Public Health, Tianjin Medical University, Tianjin, China. fangzhongze@tmu.edu.cn (Z.-Z. Fang).

Conflict of interest statement

The authors have declared that there are no conflicts of interest.

Appendix A. Supplementary data

Supplementary data related to this article can be found at http://dx.doi.org/10.1016/j.chemosphere.2017.07.105.

BBZP-UGT2B4, respectively. In conclusion, exposure to PAEs might influence the metabolic elimination of endogenous compounds and xenobiotics through inhibiting UGTs.

GRAPHICAL ABSTRACT

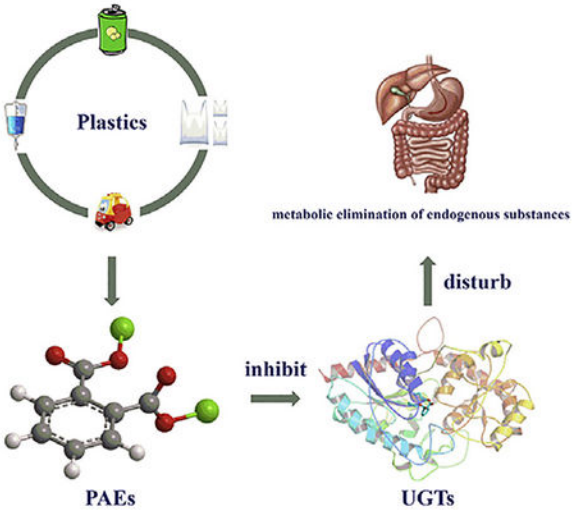

Keywords

Phthalate esters; Uridine diphosphate; glucuronosyltransferases; Kinetic parameters

1. Introduction

Phthalate esters (PAEs), composed of an rigid aromatic nucleus and two side chain esters of various lengths, have been extensively used in industry as precursors for the synthesis building materials, automobile parts, electronic products, cosmetics and medical devices, notably as plasticizers to reinforce the flexibility and stretchability of plastics (Huang et al., 2012; Net et al., 2015). Because of the hydrogen bond and van der waals force (VDW) rather than covalent bonding between PAEs and plastics, PAEs can slowly leach from plastics over time to contaminate air, soil, water and food, which can result in the exposure of humans through skin, respiratory tract, digestive tract and medical injection (Wittassek et al., 2007; Bergé et al., 2013). The abbreviations and side chains of PAEs which are generally used in industry (Kamrin, 2009) are shown in Table 1.

There have been numerous studies focusing on the carcinogenicity, teratogenicity and mutagenicity of PAEs (Gardner et al., 2016; Köksal et al., 2016; Miao et al., 2017). PAEs have an adverse impact on hormone signaling and are designated endocrine disruptors. For example, there are negative correlations between PAEs and thyroxine signaling (Huang et al., 2016). In addition, maternal PAE exposure negatively correlates with the levels of reproductive hormones in fetal blood (Araki et al., 2014). They also were demonstrated to possess estrogenic endocrine disrupting activity *in vivo* (Chen et al., 2014).

The metabolism of PAE has two steps. PAEs are hydrolyzed to phthalate monoesters and the resultant monoesters can be conjugated with uridine diphosphate glucuronic acid (UDPGA) by uridine diphosphate glucuronosyltransferases (UGTs) (Harris et al., 2016). A recent study showed that UGTs play a major role in the metabolism of DEHP by catalyzing the formation of glucuronide conjugates at the following order of potency: UGT1A9 > UGT2B7 > UGT1A7 > UGT1A8 ≥ UGT1A10 > UGT1A3 > UGT2B4 (Hanioka et al., 2017). These results possible interactions between PAEs and UGTs that many influence UGT activities toward endogenous and xenobiotic compounds.

UGTs not only affect the metabolic stability of many drugs *in vivo*, but also metabolize many endogenous substances. For example, thyroid hormone is mainly catalyzed by UGT1A1 in liver, and by UGT1A8 and UGT1A10 in jejunum (Yamanaka et al., 2007). Estrogen and its metabolites are converted by UGTs to inactive glucuronides (Cheng et al., 1998). Similarly, the glucuronidation reaction catalyzed by UGTs is critical to the termination of androgen signaling (Bélanger et al., 2003). UGTs also participate in the metabolism of many other endogenous components such as bili-rubin (Bosma et al., 1994), serotonin (Krishnaswamy et al., 2003) and bile acids (Monaghan et al., 1997). Therefore, the inhibition of UGT might seriously affect the metabolism of various endogenous substances.

The aim of the present study was to investigate the potential inhibition of PAEs towards the human UGTs. Fifteen PAEs (DAP, DBP, DCHP, DEHP, DEP, DiBP, DiOP, DiPP, DMEP, DMP, DHP, DNP, DPP, BBOP and BBZP) were tested on 11 recombinant human UGTs (UGT1A1, 1A3, 1A6, 1A7, 1A8, 1A9, 1A10, 2B4, 2B7, 2B15 and 2B17). Furthermore, enzyme kinetics and *in silico* docking experiments were carried out to explain at the molecular level, the kinetic relationship between PAEs and UGTs.

2. Materials and methods

2.1. Chemicals and reagents

PAEs were purchased from J&K Chemical (Beijing, China). Recombinant human UGT isoforms (UGT1A1, UGT1A3, UGT1A6, UGT1A7, UGT1A8, UGT1A9, UGT1A10, UGT2B4, UGT-2B7, UGT2B15 and UGT2B17) expressed in baculovirus-infected insect cells were purchased from BD Gentest Corp. (Woburn, MA, US). 4-Methylumbelliferone (4-MU), UDPGA (Trisodium salt), Tris-HCl, $MgCl_2$ and 7-hydroxycoumarin were purchased from Sigma-Aldrich (St. Louis, MO, US). Millipore Elix 5 UV and Milli-Q Gradient Ultra-Pure Water System was used to make ultra-pure water. All other reagents were of high-performance liquid chromatography (HPLC) grade or of the highest grade commercially available.

2.2. Preliminary screening of PAEs using in vitro incubation

4-MU was used as a nonselective probe substrate for recombinant UGTs to determine the inhibition of PAEs (Liu et al., 2016). The incubation system (Chen et al., 2017) containing 100 μM PAEs, 50 mM Tris-HCl buffer (pH 7.4) and 5 mM $MgCl_2$ in a total volume of 200 μL, was prepared, in which different concentrations of 4-MU (110, 1200, 110, 30, 750, 30, 30, 1000, 350, 250 and 2000 μM 4-MU) and 0.125, 0.05, 0.025, 0.05, 0.025, 0.05, 0.05,

0.25, 0.05, 0.2 and 0.5 mg/ml of UGT1A1, UGT1A3, UGT1A6, UGT1A7, UGT1A8, UGT1A9, UGT1A10, UGT2B4, UGT2B7, UGT2B15 and UGT2B17, respectively were incubated together to ensure that the reaction rates were within the linear range. Incubations without PAEs were used as controls. After a preincubation at 37 °C for 5 min, 5 mM UDPGA was added to initiate the incubation reactions. The reactions were quenched by the addition of 200 μL acetonitrile including 100 μM 7-hydroxycoumarin as an internal standard after 30–120 min. The mixtures were centrifuged at 10,625 g for 10 min to obtain the supernatant, which was then transferred to an auto-injector vial for UPLC analysis. Chromatographic separation was carried out using a C18 column (4.6 × 200 mm, 5 μm, Kromasil) at a flow rate of 0.2 mL/min and UV detector at 316 nm. The mobile phase consisted of H_2O containing 0.5% (v/v) formic acid (A) and acetonitrile (B). The following gradient condition was applied: 0–3.50 min, 90% A and 10% B; 3.50–4.00 min, 35% A and 65% B; 4.01–7.00 min, 90% A and 10% B. The calculation curve was generated by peak area ratio (4-MUG/internal standard) and all experiments were performed in two independent experiments in duplicate. The PAEs whose inhibition ratios to UGTs were more than 75% were screened out to proceed with the subsequent experiment.

2.3. Inhibition kinetics assay

Concentration-dependent inhibition of PAEs on the activity of UGTs was determined. PAEs at 0, 0.5, 1, 5, 10, 20, 40, 60, 80 and 100 μM, selected from preliminary screening, were prepared to determine the IC_{50}. The concentrations of PAEs whose inhibition ratios were 20%, 40%, 60% and 80% were chosen to undertake the inhibition kinetics assays. Various concentrations of 4-MU were used to determine the inhibition kinetic behaviors (including kinetic type and parameters) in the presence or absence of PAEs based on each different UGT. Lineweaver-Burk plots were applied to determine the inhibition type. Inhibition kinetic parameters (K_i) were calculated through correlating the slopes from the Lineweaver-Burk plots versus the concentrations of PAEs.

2.4. In vitro-in vivo extrapolation (IVIVE)

The extent of *in vivo* inhibition of UGTs was predicted using *in vitro-in vivo* extrapolation (IVIVE). The following equation was used:

$$AUC_i/AUC = 1 + [I]/K_i$$

The terms are defined as follows: AUC_i/AUC was the predicted ratio of *in vivo* exposure of xenobiotics or endogenous substances with or without the co-exposure of PAEs. [I] was the *in vivo* exposure concentration of PAEs, and the K_i was *in vitro* inhibition constant. The standard was as followed: $[I]/K_i < 0.1$, low possible; $0.1<[I]/K_i < 1$, medium possible; $[I]/K_i > 1$, high possible.

2.5. In silico docking to explain the inhibition of PAEs on UGTs activities

To understand the interaction mechanism of PAEs on UGTs, *in silico* docking method was used to dock the chemical structure of PAEs into the activity cavity of UGTs. Homology modeling was used to build 3D structure of UGTs. Autodock Version 4.2 was employed to

dock the flexible small molecule of PAEs into the rigid protein of UGTs. The non-polar hydrogen atoms of UGTs enzyme were merged. The gridbox was generated with 50 × 50 × 50 in X,Y and Z coordinate, and the grid point spacing was set to 0.375 Å. Lamarckian Genetic Algorithm (LGA) method was selected to possess molecular docking study for the binding of PAEs towards UGTs. The interactions between PAEs and UGTs were analyzed, including hydrogen bonds and hydrophobic contacts.

3. Results

3.1. Inhibition potential of PAEs towards UGT isoforms

The inhibition ratios of PAEs towards various UGT isoforms are shown in Fig. 1 and Supplemental Fig. 1A–1G and. One-hundred micromole PAEs exhibited weak inhibition towards the activity of UGT1A1, UGT1A3, UGT1A8, UGT1A10, UGT2B7, UGT2B15 and UGT2B17 by reducing the glucuronidation to less than 75% (Supplemental Fig. 1A–1G). The activity of UGT1A6 was inhibited by 74.3% and 79.3% at 100 μM of BBZP ($p < 0.05$) and BBOP ($p < 0.05$), but slightly inhibited by all the other PAEs. Similarly, PAEs showed limited inhibition of UGT1A7 and UGT2B4, with inhibition of 78.5% and 79.6% by BBZP and BBOP, respectively, toward UGT1A7, and 92.9%, 88.8%, 86.9%, 85.4% by DiBP, BBZP, DBP, DAP toward UGT2B4, respectively. Unlike the other UGTs, UGT1A9 was broadly inhibited by DCHP, BBZP, DiBP, DiPP, DBP, DPP, BBOP, DnHP and DMEP, with the reductions of 4-MU glucuronidation activity by97.0%, 93.6%, 89.8%, 88.9%, 87.0%, 84.09%, 83.8%, 82.7% and 80.4%, respectively.

3.2. Inhibition kinetic analysis

The concentration-dependent inhibition of PAEs towards UGT isoforms was exhibited. The IC_{50} values for the inhibition BBOP and BBZP towards UGT1A6 were 35.1 and 53.2 μM (Fig. 2, Table 2); IC_{50} values for the inhibition of BBOP and BBZP towards UGT1A7 were18.2 and 19.5 μM (Fig. 3, Table 2); IC_{50} values for the inhibition of DiPP, DiBP, DCHP, DBP, BBZP, BBOP, DMEP, DPP and DHP towards UGT1A9 were 14.7, 7.0, 1.5, 17.6, 5.5, 28.3, 18.3, 18.5 and 25.4 μM (Fig. 4, Table 2); IC_{50} values for the inhibition of DiBP, DBP, DAP and BBZP towards UGT2B4 were 5.9, 11.9, 14.3 and 13.8 μM (Fig. 5, Table 2).

Furthermore, inhibition kinetics were determined, including kinetic type and parameters (Ki). Both BBOP and BBZP exhibited noncompetitive inhibition towards UGT1A6. Both BBOP and BBZP exhibited competitive inhibition towards UGT1A7. BBOP exerted noncompetitive inhibition towards UGT1A9, while other PAEs showed competitive inhibition towards UGT1A9, including DCHP, BBZP, DiBP, DiPP, DBP, DPP, DnHP, and DMEP. The inhibition of BBZP, DiBP, and DBP towards UGT2B4 was noncompetitive while DAP showed competitive inhibition on UGT2B4. The inhibition kinetic parameters (Ki) were 15.5, 52.3, 23.6, 12.3, 5.6, 2.8, 1.1, 22.8, 0.8,73.7, 4.5, 1.7, 0.6, 6.8, 4.9, 6.7, and 7.2 μM for BBOP-UGT1A6, BBZPUGT1A6, BBOP-UGT1A7, BBZP-UGT1A7, DiPP-UGT1A9, DiBPUGT1A9, DCHP-UGT1A9, DBP-UGT1A9, BBZP-UGT1A9, BBOPUGT1A9, DMEP-UGT1A9, DPP-UGT1A9, DHP-UGT1A9, DiBPUGT2B4, DBP-UGT2B4, DAP-UGT2B4, and BBZP-UGT2B4, respectively (Table 2). The representative data are shown in Fig. 6 in which the Lineweaver-Burk plot (Fig. 6A) and the secondary plot

(Fig. 6B) are shown for inhibition of BBZP towards UGT1A9. The Lineweaver-Burk and second plot for the inhibition of other PAEs towards different UGTs are given in Supplemental Fig. 2A–2P.

3.3. Molecular docking of PAEs towards UGT1A9

Because PAEs showed broad inhibition on UGT1A9, the mechanism analysis for the inhibition of PAEs towards UGT1A9 was performed using *in silico* docking methods. Homology modeling was carried out to construct the crystal structure of UGT1A9, and the chemical structures of PAEs were docked into the activity cavities of UGT1A9 using *in silico* docking method. Representative docking results are shown for BBZP. The active site of UGT1A9 binding with BBZP was composed of amino acids residues PHE-14, THR-15, TYR-52, ASN-251, CYS-252, LEU-258, PRO-259, ARG-308, TRP-326, LEU-327, PRO-328, GLN-329, ASN-330, HIS-348 and GLU-352 (Fig. 7). In the binding pocket of UGT1A9, BBZP formed three hydrogen bonds to GLN-329 and ASN-330 (Fig. 8). BBZP formed hydrophobic contacts with amino acids residues PHE-14, ASN-251, CYS-252, PRO-259, TRP-326, LEU-327, PRO-328 and GLU-352 in the active pocket of UGT1A9 (Fig. 9). The other molecular docking results are shown in Supplementary 3A–H, 4A–H, and 5A–H. The binding free energy of BBZP, BBOP, DCHP, DiBP, DiPP, DBP, DPP, DHP and DMEP towards UGT1A9 was −6.53, −5.84, −7.52, −5.81, −5.79, −5.61, −5.77, −6.10 and −4.75 kcal/mol, respectively.

4. Discussion

An *in vitro* incubation system was used to determine the inhibition potential of PAEs towards the activity of 11 human UGTs, and the results indicated that some PAEs exhibited strong inhibition toward UGT1A6, UGT1A7, UGT1A9 and UGT2B4. UGT1A6 catalyzes the conjugation 5-HT, an important neurotransmitter (Krishnaswamy et al., 2003), UGT1A7 and UGT1A9 are the main metabolic enzymes of thyroxine conjugation (Yamanaka et al., 2007), and UGT2B4 is involved in the conjugation of bile acids (Barbier et al., 2003). Therefore, concentrations of these vital endogenous compounds could be affected by PAEs inhibition of these UGTs.

The structure specificity of PAEs showed a broad inhibition of UGT1A6, UGT1A7, UGT1A9 and UGT2B4 by BBZP, that is converted to monobenzyl phthalate (MBZP) and then conjugated UGTs. Other prominent inhibitors of UGTs such as BBOP and DBP had a similar glucuronidation metabolic elimination pathway (Silva et al., 2003). In contrast, PAEs with short chains like DEP, that are converted to MEP and not significantly conjugated by UGTs (Silva et al., 2003), showed a slight inhibition to all UGTs. DEHP, that is metabolized to mono (2-ethylhexyl) phthalate (MEHP), mono (2-ethyl-5-hydroxyhexyl) phthalate (MEHHP), mono (2-ethyl-5-oxohexyl) phthalate (MEOHP), mono (2-ethyl-5-carboxypentyl) phthalate (MECPP) and mono (2-carboxymethylhexyl) phthalate (MCMHP), also showed a weak inhibition towards UGTs (Silva et al., 2006). Therefore, the present results revealed the preliminary structure-activity relationships for the inhibition of PAEs towards UGT isoforms: 1) PAEs with long chains exhibited that are more extensively metabolized, exhibited stronger inhibition towards UGTs; 2) PAEs with a single metabolic

pathway exhibited stronger inhibition towards UGTs; 3) UGT1A9 was the most vulnerable to the inhibition of PAEs.

In vitro-in vivo extrapolation (IVIVE) was carried out to predict *in vivo* inhibition magnitude. According to $[I]/K_i$ ratio ($[I]/K_i > 0.1$) evaluation standard, the threshold value for inducing *in vivo* inhibition was calculated to be 1.6, 5.2, 2.4, 1.2, 0.6, 0.3, 0.1, 2.3, 0.08, 7.4,0.5, 0.2, 0.06, 0.7, 0.5, 0.7, and 0.7 μM for BBOP-UGT1A6, BBZPUGT1A6, BBOP-UGT1A7, BBZP-UGT1A7, DiPP-UGT1A9, DiBPUGT1A9, DCHP-UGT1A9, DBP-UGT1A9, BBZP-UGT1A9, BBOPUGT1A9, DMEP-UGT1A9, DPP-UGT1A9, DHP-UGT1A9, DiBPUGT2B4, DBP-UGT2B4, DAP-UGT2B4, and BBZP-UGT2B4, respectively. A statistical study of PAEs was used to show that the plasma concentrations of total PAEs was approximately 85.0 ng/mL in humans (Wan et al., 2013). Based on this value, the *in vivo* exposure concentration was calculated to be approximately 0.3 μM, which exceeds the threshold value for most PAEs. Therefore, the exposure of PAEs might disturb the metabolic elimination of endogenous compounds through inhibiting UGTs *in vivo*.

In conclusion, the inhibition profiles of PAEs on human UGTs was investigated in the present study. PAEs exhibited no significant inhibition on the activity of UGT1A1, UGT1A3, UGT1A8, UGT1A10, UGT2B15, and UGT2B17. PAEs showed limited inhibition of UGT1A6, UGT1A7 and UGT2B4, and UGT1A9 was broadly inhibited by PAEs. The inhibition kinetics was determined for the inhibition of PAEs toward UGTs, and *in silico* docking of PAEs toward UGT1A9 was performed. This study suggest that the influence of PAEs towards UGTs' activity and their potential effects on endogenous hormone signaling and drug therapy should be monitored.

Supplementary Material

Refer to Web version on PubMed Central for supplementary material.

Acknowledgement

This work was supported by the project for the National Key Research and Development Program (2016YFC0903100, 2016YFC0903102), The 13th five year plan and TMU talent project (11601501/2016KJ0313), National Natural Science Foundation of China (No. 81602826, 81672961), individualized diagnosis and treatment of colorectal cancer (No. LNCCC-B05–2015), Foundation of Committee on Science and Technology of Tianjin (Grant No. 15JCYBJC54700), the China Postdoctoral Science Foundation (2016M590210), Tianjin Health Bureau Science Foundation Key Project (16KG154) and Tianjin Project of Thousand Youth Talents.

References

Araki A, Mitsui T, Miyashita C, Nakajima T, Naito H, Ito S, Sasaki S, Cho K, Ikeno T, Nonomura K, 2014 Association between maternal exposure to di (2-ethylhexyl) phthalate and reproductive hormone levels in fetal blood: the Hokkaido study on environment and children's health. Plos One 9, e109039. [PubMed: 25296284]

Barbier O, Duran-Sandoval D, Pineda-Torra I, Kosykh V, Fruchart J, Staels B, 2003 Peroxisome proliferator-activated receptor a induces hepatic expression of the human bile acid glucuronidating UDP-glucuronosyltransferase 2B4 enzyme. J. Biol. Chem 278, 32852–32860. [PubMed: 12810707]

Bélanger A, Pelletier G, Labrie F, Barbier O, Chouinard S, 2003 Inactivation of androgens by UDP-glucuronosyltransferase enzymes in humans. Trends Endocrinol. Metabol 14, 473–479.

Bergé A, Cladière M, Gasperi J, Coursimault A, Tassin B, Moilleron R, 2013 Meta-analysis of environmental contamination by phthalates. Environ. Sci. Pollut. R 20, 8057–8076.

Bosma PJ, Seppen J, Goldhoorn B, Bakker C, Elferink RO, Chowdhury JR, Chowdhury NR, Jansen PL, 1994 Bilirubin UDP-glucuronosyltransferase 1 is the only relevant bilirubin glucuronidating isoform in man. J. Biol. Chem 269, 17960–17964. [PubMed: 8027054]

Chen D, Du Z, Zhang C, Zhang W, Cao Y, Sun H, Zhu Z, Yang K, Liu Y, Zhao Z, 2017 The inhibition of UDP-glucuronosyltransferases (UGTs) by tetraiodothyronine (T4) and triiodothyronine (T3). Xenobiotica 1–18.

Chen X, Xu S, Tan T, Lee ST, Cheng SH, Lee FWF, Xu SJL, Ho KC, 2014 Toxicity and estrogenic endocrine disrupting activity of phthalates and their mixtures. Int. J. Env. Res. Pub. HE 11, 3156–3168.

Cheng Z, Rios GR, King CD, Coffman BL, Green MD, Mojarrabi B, Mackenzie PI, Tephly TR, 1998 Glucuronidation of catechol estrogens by expressed human UDP-glucuronosyltransferases (UGTs) 1A1, 1A3, and 2B7. Toxicol. Sci 45, 52–57. [PubMed: 9848110]

Gardner ST, Wood AT, Lester R, Onkst PE, Burnham N, Perygin DH, Rayburn J, 2016 Assessing differences in toxicity and teratogenicity of three phthalates, Diethyl phthalate, Di-n-propyl phthalate, and Di-n-butyl phthalate, using Xenopus laevis embryos. J. Toxicol. Environ. Health, Part A 79, 71e82. [PubMed: 26730679]

Hanioka N, Kinashi Y, Tanaka-Kagawa T, Isobe T, Jinno H, 2017 Glucuronidation of mono(2-ethylhexyl) phthalate in humans: roles of hepatic and intestinal UDP-glucuronosyltransferases. Arch. Toxicol 91, 689–698. [PubMed: 27071666]

Harris S, Wegner S, Hong SW, Faustman EM, 2016 Phthalate metabolism and kinetics in an in vitro model of testis development. Toxicol. Vitro 32, 123–131.

Huang P, Liou S, Ho I, Chiang H, 2012 Phthalates exposure and endocrinal effects: an epidemiological review. J. Food Drug Anal 20.

Huang P, Tsai C, Liang W, Li S, Huang H, Kuo P, 2016 Early phthalates exposure in pregnant women is associated with alteration of thyroid hormones. Plos One 11, e159398.

Kamrin MA, 2009 Phthalate risks, phthalate regulation, and public health: a review. J. Toxicol. Environ. Health, Part B 12, 157–174.

Köksal Ç, Nalbantsoy A, Yavaşoğlu NÜK, 2016 Cytotoxicity and genotoxicity of butyl cyclohexyl phthalate. Cytotechnology 68, 213–222. [PubMed: 25501535]

Krishnaswamy S, Duan SX, von Moltke LL, Greenblatt DJ, 2003 Validation of serotonin (5-hydroxtryptamine) as an in vitro substrate probe for human UDP-glucuronosyltransferase (UGT) 1A6. Drug Metab. Dispos 31, 133–139. [PubMed: 12485962]

Liu X, Cao Y, Ran R, Dong P, Gonzalez FJ, Wu X, Huang T, Chen J, Fu Z, Li R, 2016 New insights into the risk of phthalates: inhibition of UDP-glucuronosyltransferases. Chemosphere 144, 1966–1972. [PubMed: 26547877]

Miao Y, Wang R, Lu C, Zhao J, Deng Q, 2017 Lifetime cancer risk assessment for inhalation exposure to di (2-ethylhexyl) phthalate (DEHP). Environ. Sci. Pollut. R 24, 312–320.

Monaghan G, Burchell B, Boxer M, 1997 Structure of the human UGT2B4 gene encoding a bile acid UDP-glucuronosyltransferase. Mamm. GENOME 8, 692–694. [PubMed: 9271674]

Net S, Delmont A, Sempéré R, Paluselli A, Ouddane B, 2015 Reliable quantification of phthalates in environmental matrices (air, water, sludge, sediment and soil): a review. Sci. Total Environ 515, 162–180. [PubMed: 25723871]

Silva MJ, Barr DB, Reidy JA, Kato K, Malek NA, Hodge CC, Hurtz D, Calafat AM, Needham LL, Brock JW, 2003 Glucuronidation patterns of common urinary and serum monoester phthalate metabolites. Arch. Toxicol 77, 561–567. [PubMed: 14574443]

Silva MJ, Reidy JA, Preau JL, Jr., Samandar E, Needham LL, Calafat AM, 2006 Measurement of eight urinary metabolites of di (2-ethylhexyl) phthalate as biomarkers for human exposure assessment. Biomarkers 11, 1–13. [PubMed: 16484133]

Wan HT, Leung PY, Zhao YG, Wei X, Wong MH, Wong CK, 2013 Blood plasma concentrations of endocrine disrupting chemicals in Hong Kong populations. J. Hazard Mater 261, 763–769. [PubMed: 23411151]

Wittassek M, Wiesmüller GA, Koch HM, Eckard R, Dobler L, Müller J, Angerer J, Schlüter C, 2007 Internal phthalate exposure over the last two decadesea retrospective human biomonitoring study. Int. J. Hyg. Environ. Heal 210, 319–333.

Yamanaka H, Nakajima M, Katoh M, Yokoi T, 2007 Glucuronidation of thyroxine in human liver, jejunum, and kidney microsomes. DRUG Metab. Dispos 35, 1642–1648. [PubMed: 17591679]

HIGHLIGHTS

- PAE showed broad inhibition on the activity of UGT1A9.
- Hydrogen bonds and hydrophobic interaction contribute to the inhibition of PAEs towards UGT1A9.
- Threshold value for PAEs' inhibition towards UGTs was obtained.

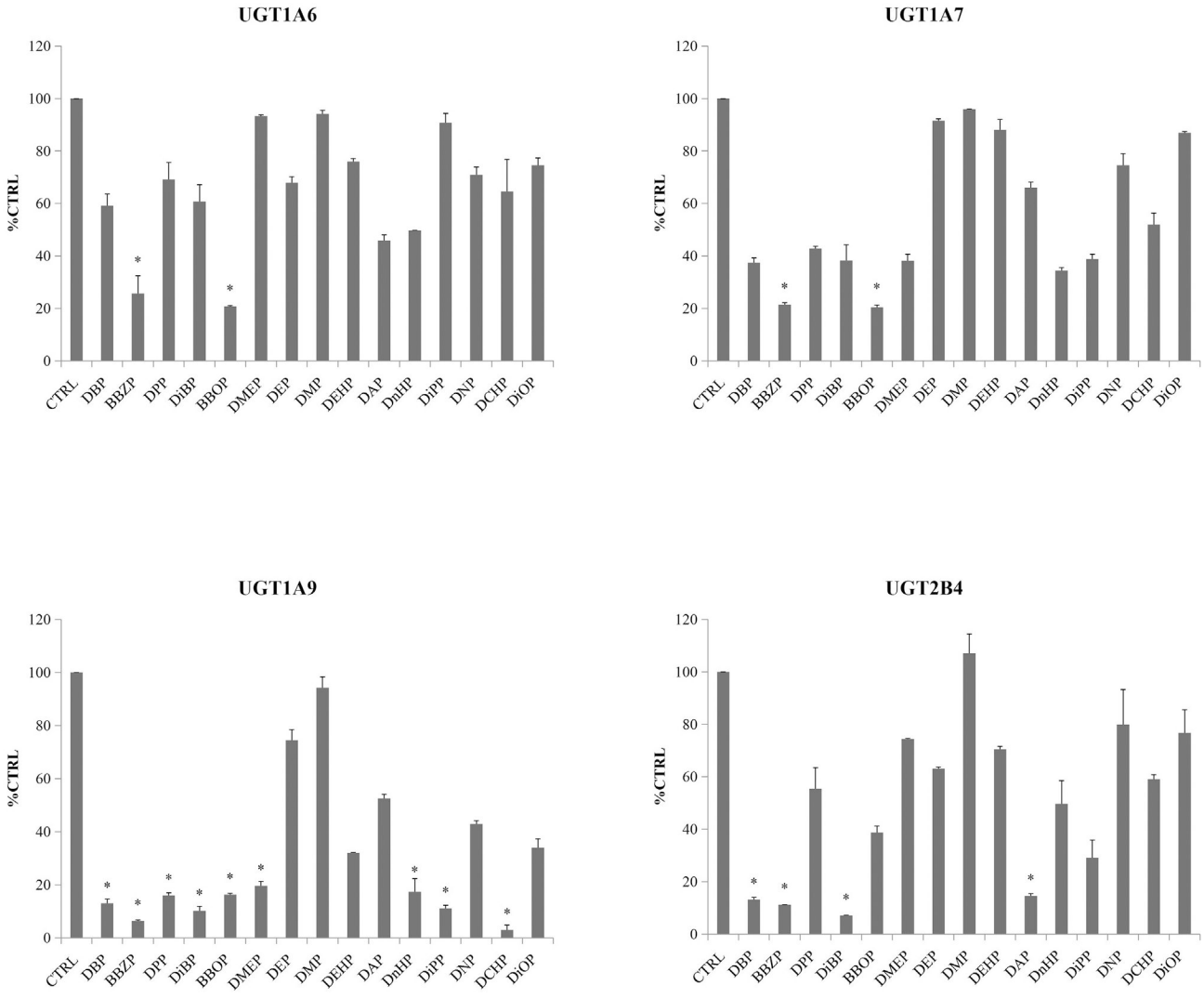

Fig. 1.

Inhibition potential of DBP, BBZP, DPP, DiBP, BBOP, DMEP, DEP, DMP, DEHP, DAP, DnHP, DiPP, DNP, DCHP and DiOP towards UGT1A6, UGT1A7, UGT1A9 and UGT2B4. The residual activity of recombinant UGT1A1 was given, and calculated using the following equations: Residual activity (% CTRL) = the activity at 100 μM of PAEs*100%/the activity at 0 μM of PAEs. Data were presented as the mean value plus S.D.. *, $p < 0.05$.

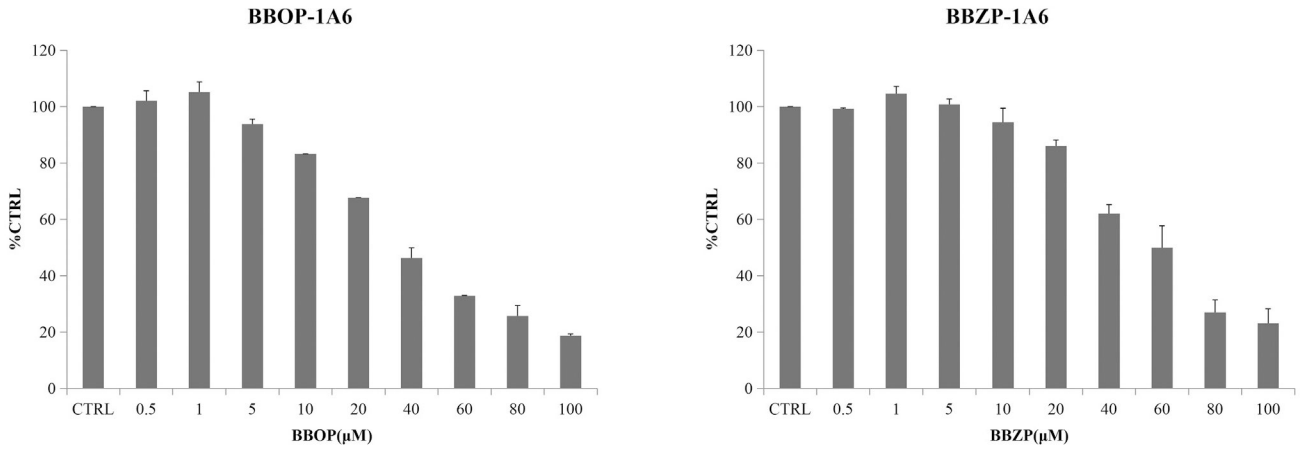

Fig. 2.

Inhibitory effects of BBOP and BBZP on UGT1A6 activity in human cDNA-expressed UGT1A6 supersomes. IC_{50} values of BBOP and BBZP towards UGT1A6 were calculated to be 35.1 and 53.2 μM, respectively. Data were presented as the mean value plus S.D..

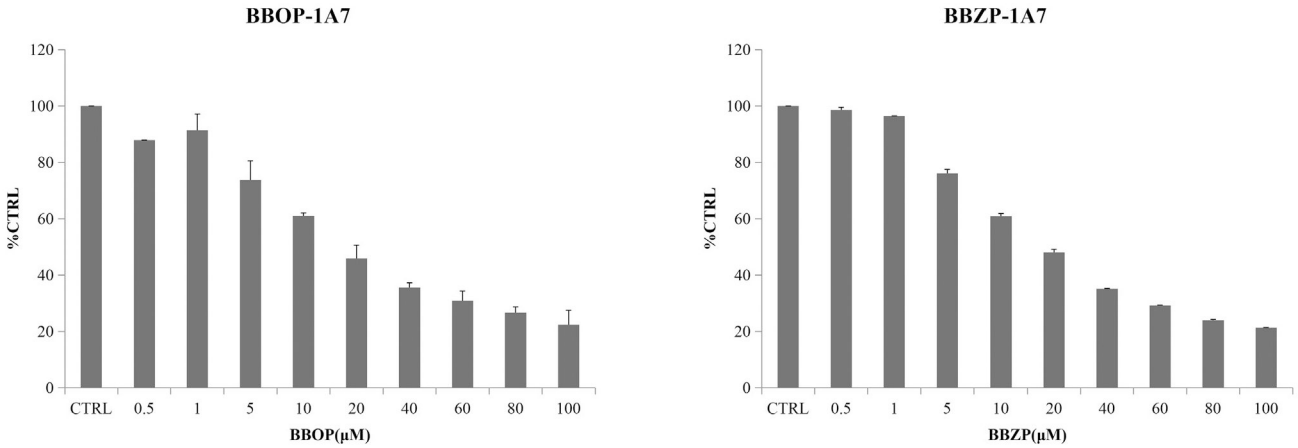

Fig. 3.

Inhibitory effects of BBOP and BBZP on UGT1A7 activity in human cDNA-expressed UGT1A7 supersomes. IC_{50} values of BBOP and BBZP towards UGT1A7 were calculated to be 18.2 and 19.5 μM, respectively. Data were presented as the mean value plus S.D..

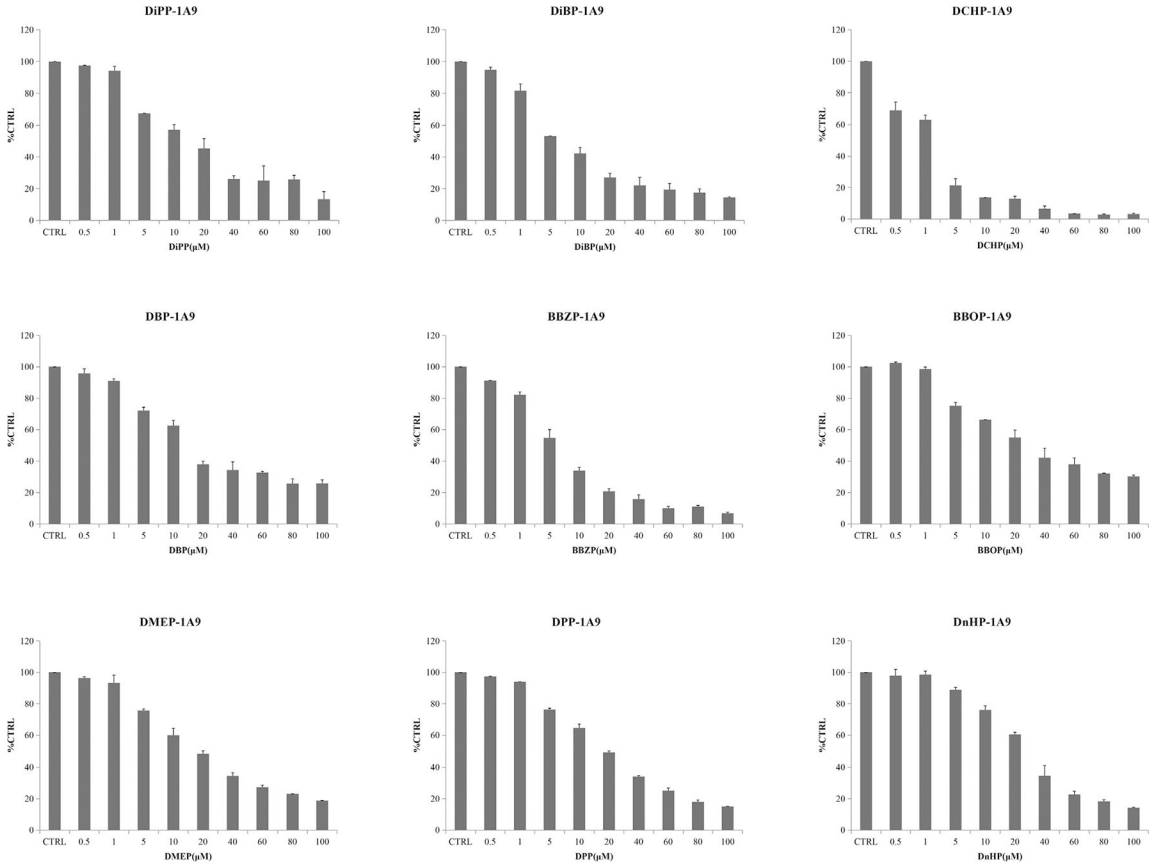

Fig. 4.

Inhibitory effects of DiPP, DiBP, DCHP, DBP, BBZP, BBOP, DMEP, DPP and DHP on UGT1A9 activity in human cDNA-expressed UGT1A9 supersomes. IC_{50} values of DiPP, DiBP, DCHP, DBP, BBZP, BBOP, DMEP, DPP and DHP on UGT1A9 were calculated to be 14.70, 7.03, 1.46, 17.6, 5.54, 28.3, 18.2, 18.5 and 25.4 mM, respectively. Data were presented as the mean value plus S.D..

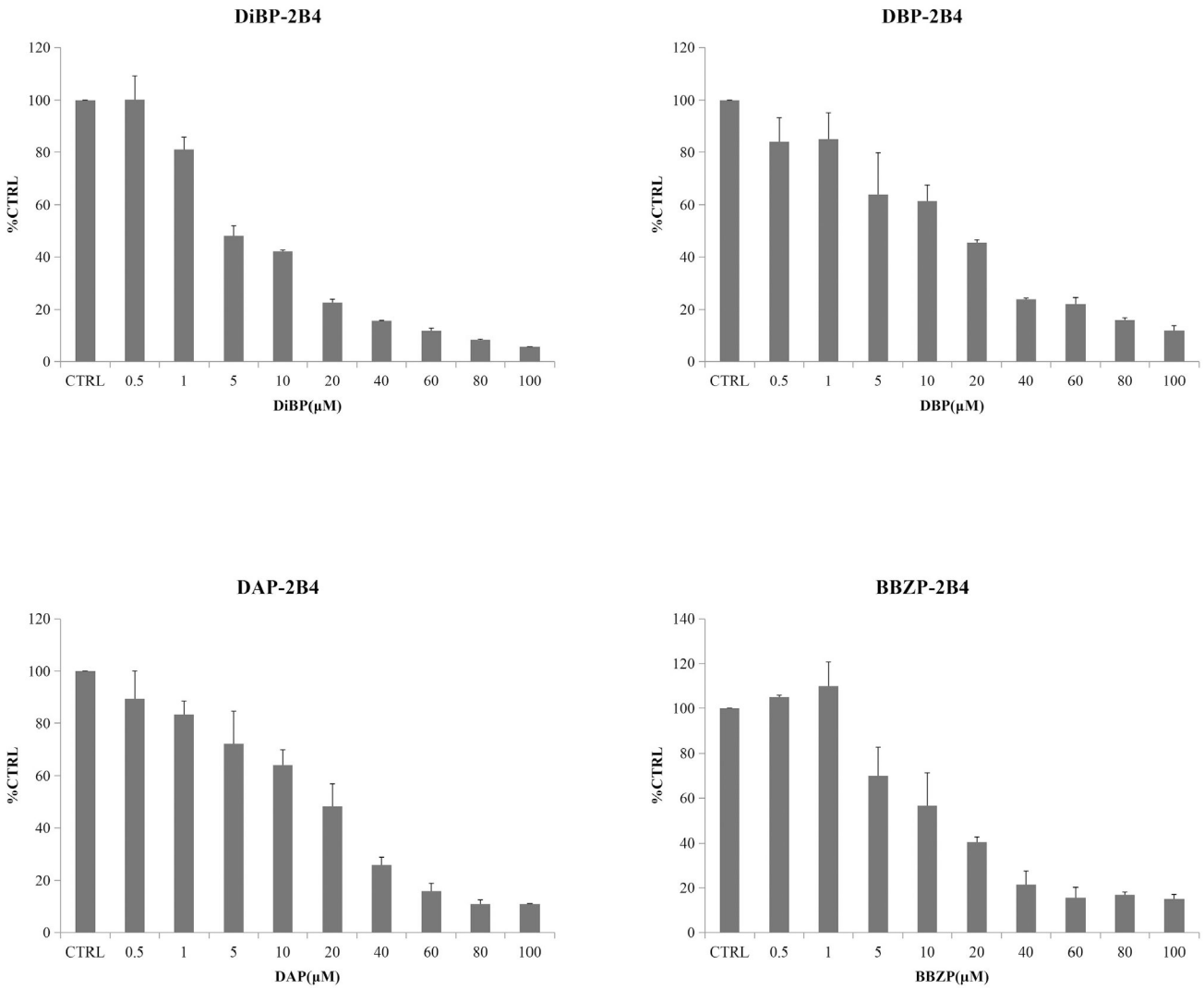

Fig. 5.

Inhibitory effects of DiBP, DBP, DAP and BBZP on UGT2B4 activity in human cDNA-expressed UGT2B4 supersomes. IC_{50} values of DiBP, DBP, DAP and BBZP on UGT2B4 were calculated to be 5.89, 11.9, 14.3 and 13.8 μM, respectively. Data were presented as the mean value plus S.D..

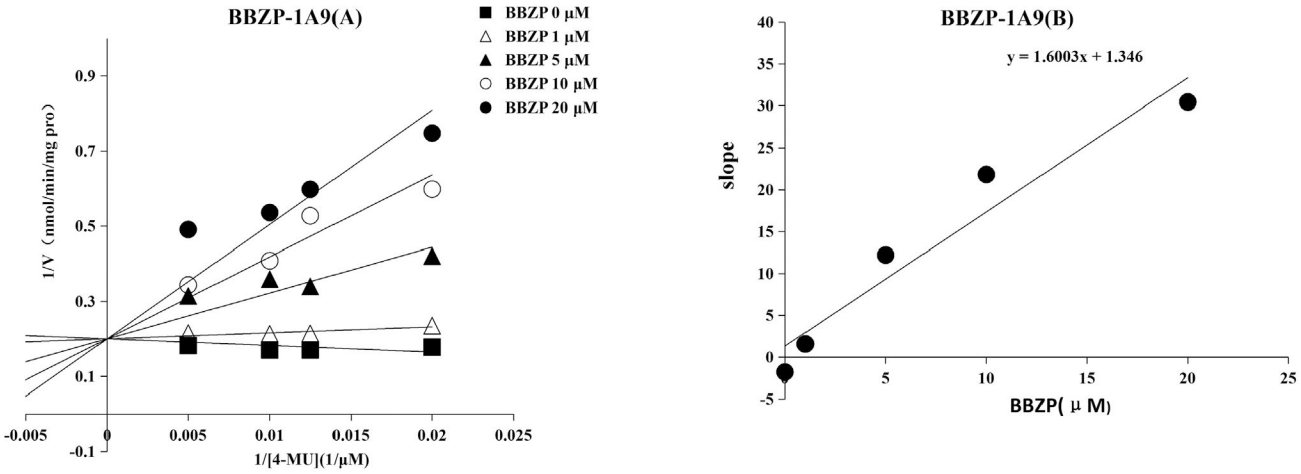

Fig. 6.

Inhibition kinetics of BBZP on UGT1A9. (A) Lineweaver-Burk plot of the inhibition of BBZP on the activity of UGT1A9. Each data point represents the mean value of duplicate experiments. (B) Determination of inhibition kinetic parameter (K_i) of BBZP on the activity of UGT1A9. The verticle axis represents the slopes of the lines from Lineweaver-Burk plot, and the horizontal axis represents the concentrations of BBZP.

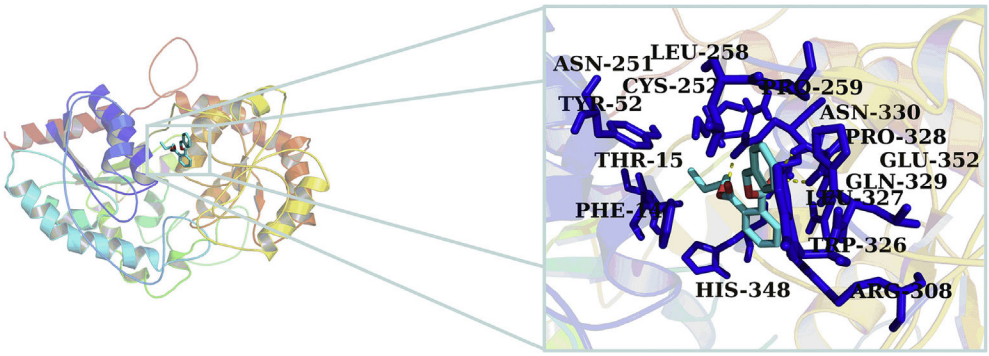

Fig. 7.

Activity pocket of UGT1A9 binding with BBZP. The active site of UGT1A9 binding with BBZP was composed of amino acids residues PHE-14, THR-15, TYR-52, ASN-251, CYS-252, LEU-258, PRO-259, ARG-308, TRP-326, LEU-327, PRO-328, GLN-329, ASN-330, HIS-348 and GLU-352.

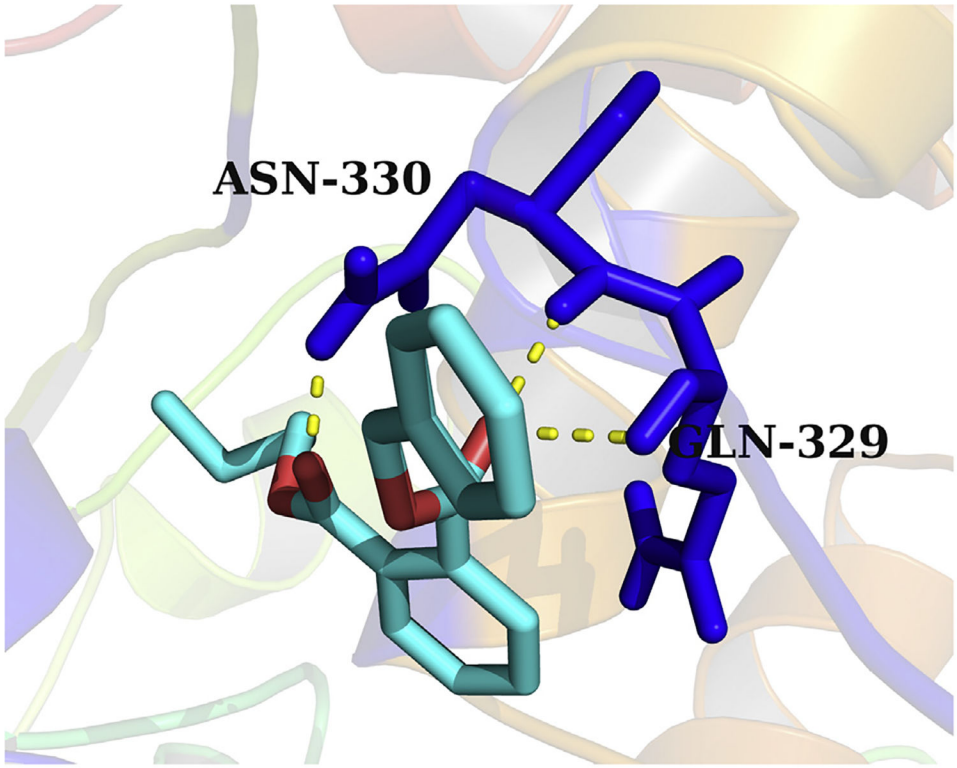

Fig. 8.

Hydrogen bonds interaction between BBZP with the activity cavity of UGT1A9. In the binding pocket of UGT1A9, BBZP formed three hydrogen bonds to GLN-329 and ASN-330.

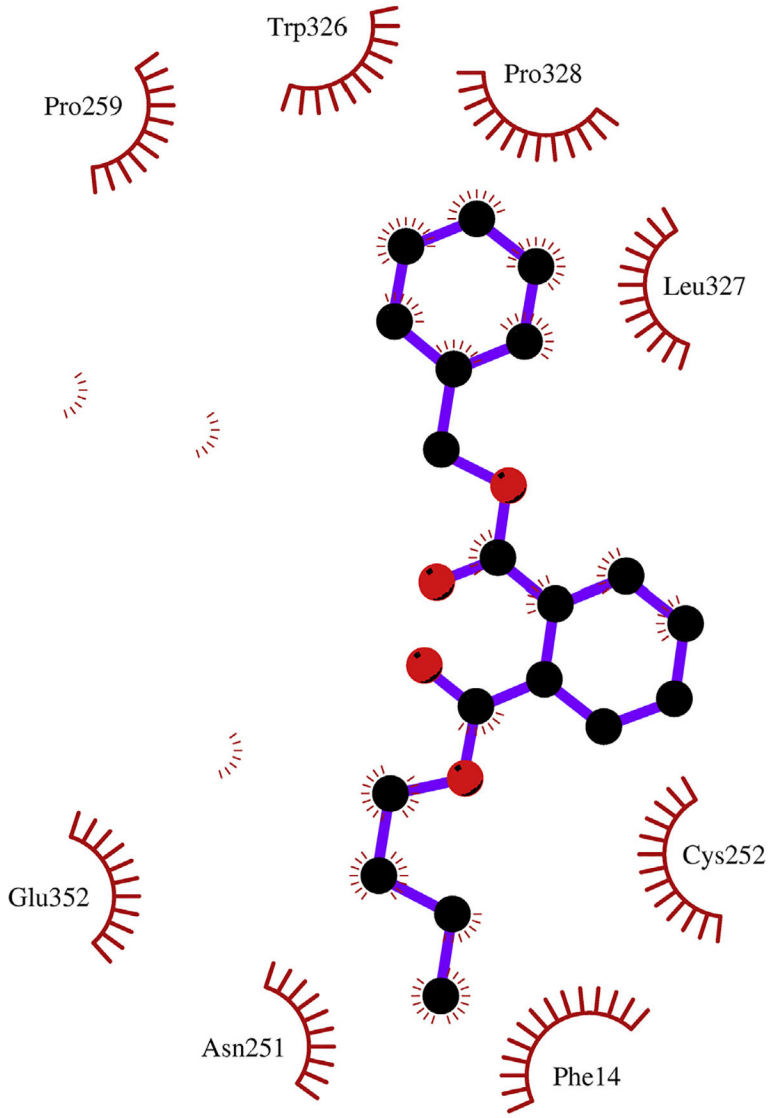

Fig. 9.

Hydrophobic interaction between BBZP and the activity cavity of UGT1A9. BBZP formed hydrophobic contacts with amino acids residues PHE-14, ASN-251, CYS-252, PRO-259, TRP-326, LEU-327, PRO-328 and GLU-352 in the active pocket of UGT1A9.

Table 1

The abbreviations and side chains of PAEs.

Name	Abbreviation	Side chains
Diallyl phthalate	DAP	Allyl
Dibutyl phthalate	DBP	Butyl
Dicyclohexyl phthalate	DCHP	Cyclohexyl
Di-2-ethylhexyl phthalate	DEHP	2-Ethylhexyl
Diethyl phthalate	DEP	Ethyl
Diisobutyl phthalate	DiBP	Isobutyl
Diisooctyl phthalate	DiOP	Isooctyl
Diisopentyl phthalate	DiPP	Isopentyl
Dimethoxyethyl phthalate	DMEP	Methoxyethyl
Dimethyl phthalate	DMP	Methyl
Dihexyl phthalate	DHP	Hexyl
Dinonyl phthalate	DNP	Nonyl
Dipentyl phthalate	DPP	Pentyl
Bis-2-Butoxyethyl Phthalate	BBOP	2-Butoxyethyl
Butyl benzyl phthalate	BBZP	Butyl/Benzyl

Table 2

The inhibition kinetics of PAEs to UGTs, including IC_{50}, inhibition kinetic type and parameters.

PAEs-UGTs	IC_{50}(μM)	inhibition type	Ki (μM)
BBOP-UGT1A6	35.1	noncompetitive	15.5
BBZP-UGT1A6	53.2	noncompetitive	52.3
BBOP-UGT1A7	18.2	competitive	23.6
BBZP-UGT1A7	19.5	competitive	12.2
DiPP-UGT1A9	14.7	competitive	5.61
DiBP-UGT1A9	7.03	competitive	2.79
DCHP-UGT1A9	1.46	competitive	1.07
DBP-UGT1A9	17.6	competitive	22.8
BBZP-UGT1A9	5.54	competitive	0.84
BBOP-UGT1A9	28.3	noncompetitive	73.7
DMEP-UGT1A9	18.2	competitive	4.51
DPP-UGT1A9	18.5	competitive	1.74
DHP-UGT1A9	25.4	competitive	0.58
DiBP-UGT2B4	5.89	noncompetitive	6.79
DBP-UGT2B4	11.9	noncompetitive	4.93
DAP-UGT2B4	14.3	competitive	6.73
BBZP-UGT2B4	13.8	noncompetitive	7.23